Numerically modeling Ceres' thermal and evolutionary history using Dawn mission data and analyses to constrain possible evolutionary pathways

Gregory J. Gosselin[1] (gosselgj@dukes.jmu.edu) and R S. McGary[2]

(1) Geology and Environmental Sciences, James Madison University, 400 S. High St., Harrisonburg, VA 22801, (2) Department of Geology & Environmental Science, James Madison University, Memorial Hall 7335, MSC 6903, Harrisonburg, VA 22807

Introduction

Data collected at Ceres by the recent Dawn mission and subsequent analyses have led to a vastly improved understanding of the largest body in the asteroid belt. From more precise constraints on simple physical parameters, such as bulk density, moment of inertia, and polar/equatorial radii, to a better characterization of the surface morphology and composition from the investigation of crater images, a clearer picture of rheological and even stratigraphic constraints have emerged.

While a number of models of Ceres' geophysical evolution were developed prior to the Dawn mission, these new data and analyses provide an opportunity to conduct an investigation along these lines, which target the physical, geophysical, chemical, and morphological constraints suggested by the new data. Here, we present the initial results from a 1.5-D finite difference model that investigates the thermal history, differentiation, and evolution of Ceres. We examined the set(s) of initial and boundary conditions (time of accretion, surface temperature and origin, initial water/rock ratio, and initial composition of rock and fluids) that best explain the suite of observations collected during the Dawn mission and subsequent analyses by the scientific community.

Methods

The framework of our code (adapted from McGary, Farrell, and Sparks (2006)) was built around the spherically symmetric conservation of energy equation, and solved using the finite difference method:

$$\gamma \frac{\partial T}{\partial t} = \frac{\partial}{\partial r}\left(k \frac{\partial T}{\partial r}\right) + \rho H - L_i \rho_i \frac{\partial X_i}{\partial t} - L_s \rho_s \frac{\partial X_s}{\partial t}$$

where γ is the heat capacity per unit volume, T is temperature, t is time (My), r is radius, k is thermal conductivity, ρ is density, H is heat production, L is latent heat, and X is volume fraction.

Non-dimensionalization identified four parameters which control the evolution of Ceres:

$$D_{surf} = \frac{(T_{BB} - 273.15K)[\rho_{Ol} c_{Ol} X_{ol} + \rho_i c_i (1 - X_i)]\lambda_U}{\rho_{Ol} X_{Ol} H_U} \quad (1)$$

$$D_d = \frac{[k_{Ol} X_{Ol} + k_i (1 - X_{Ol})]}{\lambda_U R^2 [\rho_{Ol} c_{Ol} X_{Ol} + \rho_i c_i (1 - X_{Ol})]} \quad (2)$$

$$D_{Mi} = \frac{\rho_i (1 - X_{Ol}) L_i \lambda_U}{\rho_{Ol} X_{Ol} H_U} \quad (3) \qquad D_{Al} = \frac{H_{Al}}{H_U} \quad (4)$$

(1) Ratio of the difference between blackbody and melting temperature of water ice, and temperature scale.

(2) Ratio of heat production and thermal diffusion time scales.

(3) Ratio of heat necessary to melt water ice to heat generated by silicate material.

(4) Ratio of ^{26}Al and ^{238}U heating rates; varied to control for time of accretion

Results

(1) Using Dawn's shape data: comparing and contrasting radial variability

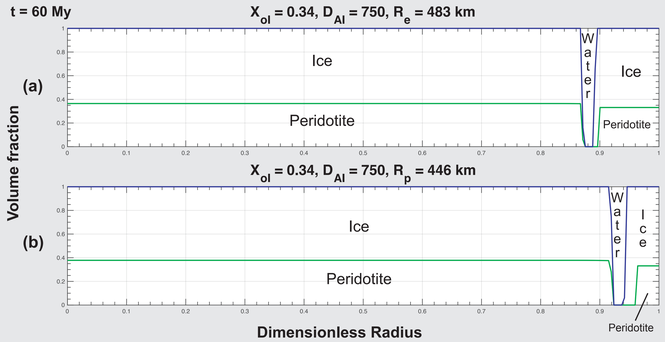

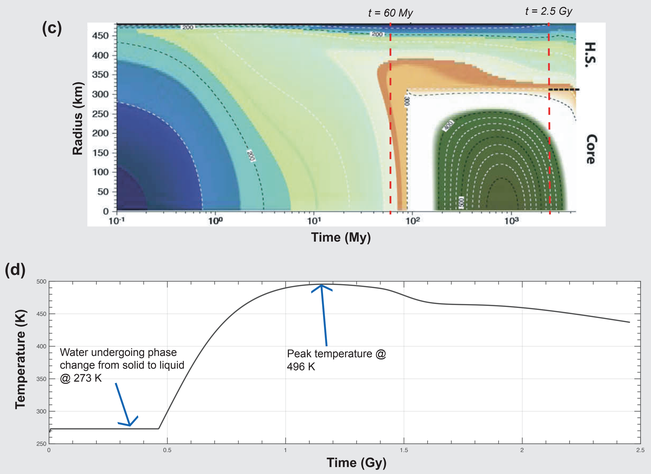

Fig. 1 - Volume fraction versus dimensionless radius at 60 My after accretion. Initial and surface temperatures are 150 K and 185 K, respectively. Initial mass fraction of silicates set to 0.65. D_{Al} corresponds to time of accretion 3.3 My after calcium-aluminum inclusions (CAIs). A marked difference in the respective locations and thicknesses of the ocean layers can be observed between the **(a)** equatorial and **(b)** polar radii. Surficial compositions are also variable in their respective thicknesses, although a trend of increased ice to peridotite volume fraction can be seen. **(c)** Figure adapted from Castillo-Rogez and McCord (2011) which contains similar initial and boundary temperature conditions, and bulk composition, although a time of accretion of 5 My after CAIs, and their model includes a salt layer. Temperature is indicated by dashed lines with 25 K interval. Vertical red dashed lines indicate 60 My and 2.5 Ga, and are coincident with the plots above **(a & b)**, and the total run time in **(d)**, respectively. The set of modeled parameters from **(a)** and **(b)** will be tested again upon inclusion of serpentinization/deserpentinization reactions, in conjunction with matching additional parameters listed above (e.g. salt layer and accretion time).

(2) Varying bulk initial composition

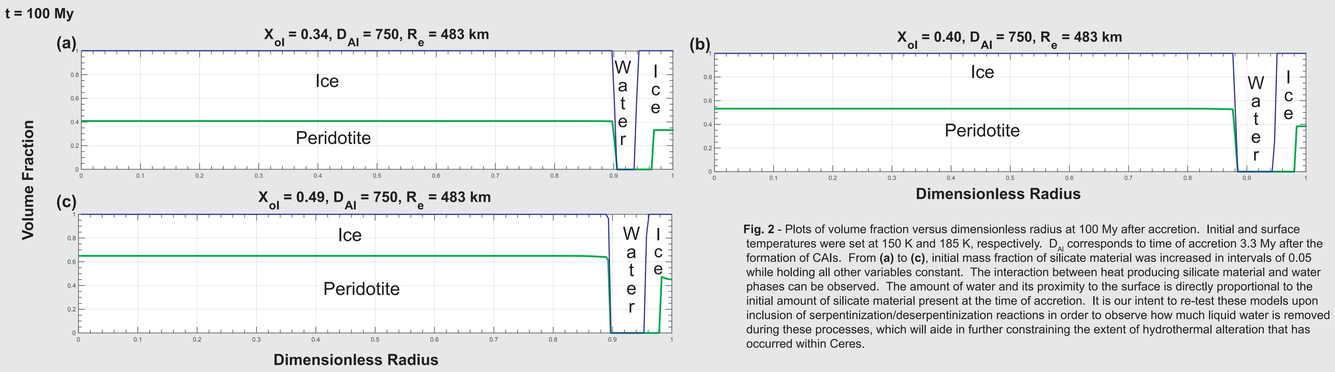

Fig. 2 - Plots of volume fraction versus dimensionless radius at 100 My after accretion. Initial and surface temperatures were set at 150 K and 185 K, respectively. D_{Al} corresponds to time of accretion 3.3 My after the formation of CAIs. From **(a)** to **(c)**, initial mass fraction of silicate material was increased in intervals of 0.05 while holding all other variables constant. The interaction between heat producing silicate material and water phases can be observed. The amount of water and its proximity to the surface is directly proportional to the initial amount of silicate material present at the time of accretion. It is our intent to re-test these models upon inclusion of serpentinization/deserpentinization reactions in order to observe how much liquid water is removed during these processes, which will aide in further constraining the extent of hydrothermal alteration that has occurred within Ceres.

(3) Late time of accretion: hydrosphere still present

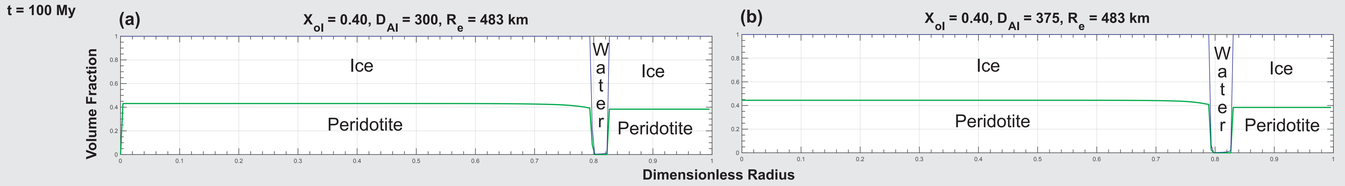

Figure 3 - Volume fraction of constituent materials versus dimensionless radius at 100 My after accretion. Initial and surface temperature were set at 150 K and 185 K, respectively. **(a)** Here, D_{Al} corresponds to a time of accretion ~4.2 My after the formation of CAIs, with an initial silicate mass fraction of 0.70. The oceanic layer is ~10 km thick, with a 386 km partially differentiated core, comprised of a rock/ice mixture. **(b)** D_{Al} corresponds to a time of accretion 4.0 My after the formation of CAIs, also with an initial silicate mass fraction of 0.70. The oceanic layer is ~14.5 km thick, with a 386 km partially differentiated core also comprised of a rock/ice mixture.

Conclusions & Further Research

- Overall, our model (Fig. 1 a & b) shows the importance of implementing Ceres' updated shape data from Dawn into existing models, such as those put forth by McCord and Sotin (2005), Castillo-Rogez and McCord (2010), and Neveu and Desch (2014, 2015).
- Difference between equatorial and polar radii yield contrasting bulk compositions at same time-slice during differentiation processes (Fig. 1).
- Extent of melting is controlled by time of accretion and, to a lesser extent, the initial amount of silicate material (Fig 1 & 2).
- Ocean layers established in all models included herein (Fig. 1, 2, & 3). Additionally, surficial composition is consistent with observed presence of water ice at Ceres' surface (Prettyman et al., 2017).

Moving forward, we plan to include and investigate the following parameters:

(1) Hydrothermal alteration of silicate material

(2) Water/antifreeze interactions (e.g. ammonia content).

(3) Determine the importance of core cracking on Ceres' evolution, proposed by Neveu, Desch, and Castillo-Rogez (2014).

(4) Investigate the hypothesis put forth by Vernazza et al. (2017) in regards to Ceres' initial location during its accretionary phase (e.g. Kuiper belt object vs. in situ)

(5) Utilize current data and observations of Ceres' gathered during the Dawn mission to constrain surficial conditions, thus providing us with a set of refined boundary conditions.

(6) Implement density model established by Park et al. (2016) to determine the validity of our models.

Acknowledgments

I would like to thank my research advisor, Dr. R McGary for his continual assistance throughout this project; James Madison University's Department of Geology & Environmental Science for their financial support in the form of a research scholarship; and Dr. Elizabeth Johnson of James Madison University for her insight regarding geochemical processes as we move forward with this project.

References

Castillo-Rogez, J.C., and McCord, T.B., 2010, Ceres' evolution and present state constrained by shape data: Icarus, v. 205, p. 443–459, doi: 10.1016/j.icarus.2009.04.008.

McCord, T.B., and Sotin, C., 2005, Ceres: Evolution and current state: Journal of Geophysical Research, v. 110, p. 1–14, doi: 10.1029/2004JE002244.

Neveu, M., Desch, S.J., and Castillo-Rogez, J.C., 2015, Core cracking and hydrothermal circulation can profoundly affect Ceres' geophysical evolution: Journal of Geophysical Research E: Planets, v. 120, p. 123–154, doi: 10.1002/2014JE004714.

Neveu, M., and Desch, S.J., 2015, Geochemistry, thermal evolution, and cryovolcanism on Ceres with a muddy ice mantle: Geophysical Research Letters, v. 42, p. 10197–10206, doi: 10.1002/2015GL066375.

Park, R.S., Konopliv, A.S., Bills, B.G., Rambaux, N., Castillo-Rogez, J.C., Raymond, C.A., Vaughan, A.T., Ermakov, A.I., Zuber, M.T., Fu, R.R., Toplis, M.J., Russell, C.T., Nathues, A., and Preusker, F., 2016, A partially differentiated interior for (1) Ceres deduced from its gravity field and shape: Nature, v. 537, p. 515–517, doi: 10.1038/nature18955.

Prettyman, T.H., Yamashita, N., Toplis, M.J., Mcsween, H.Y., Marchi, S., Feldman, W.C., Forni, O., Lawrence, D.J., Ammannito, E., Ehlmann, B.L., Sizemore, H.G., Joy, S.P., Polanskey, C.A., Rayman, M.D., et al., 2017, Extensive water ice within Ceres' aqueously altered regolith: Evidence from nuclear spectroscopy: Science, v. 355, p. 55–59, doi: 10.1126/science.aah6765.

Vernazza, P., Castillo-Rogez, J., Beck, P., Emery, J., Brunetto, R., Delbo, M., Marsset, M., Marchis, F., Groussin, O., Zanda, B., Lamy, P., Jorda, L., Mousis, O., Delsanti, A., et al., 2017, Different Origins or Different Evolutions? Decoding the Spectral Diversity Among C-Type Asteroids: The Astronomical Journal, v. 153, p. 72, doi: 10.3847/1538-3881/153/2/72.